physica status solidi pss

www.pss-journals.com

reprint

WILEY-VCH

Phys. Status Solidi C **12**, No. 12, 1376–1382 (2015) / **DOI** 10.1002/pssc.201510159

physica status solidi c
www.pss-c.com
current topics in solid state physics

Theoretical investigation of 2DEG concentration and mobility in the AlGaN/GaN heterostructures with various Al concentrations

Karine Abgaryan[*,1], **Ilya Mutigullin**[1], **and Dmitry Reviznikov**[2]

[1] Dorodnicyn Computer Center of RAS, Vavilov st. 40, 119333 Moscow, Russia
[2] Moscow Aviation Institute, Volokolamskoe Shosse 4, 125993 Moscow, Russia

Received 16 September 2015, revised 7 October 2015, accepted 9 October 2015
Published online 27 October 2015

Keywords III-V nitrides, semiconductors, heterostructures, computational modeling

[*] Corresponding author: e-mail kristal83@mail.ru

Three-scale model for the calculation of 2DEG mobility in AlGaN/GaN heterostructures developed by our group earlier was used for the investigation of the dependence of 2DEG concentration and mobility on the Al concentration in AlGaN layer. The model allows to calculate following 2DEG properties: energy levels, corresponding wavefunctions, potential energy distribution, charge carriers concentration distribution over the heterostructure. It is also possible to calculate electron mobility in 2DEG taking into account various scattering mechanisms. In the framework of this model the values of 2DEG concentration and mobility were calculated for various Al concentrations x in $Al_xGa_{1-x}N$ barrier ($0.15 \leq x \leq 1$). It is also taken into consideration that maximum barrier width should decrease with increasing Al concentration in order to allow pseudomorphic growth of barrier layer.

© 2015 WILEY-VCH Verlag GmbH & Co. KGaA, Weinheim

1 Introduction In recent years, the transport properties of two dimensional electron gas (2DEG) in AlGaN/GaN heterostructures have received a lot of research attention because of their importance to the performance of high electron mobility transistors (HEMTs). Numerous studies with various approaches to theoretical modeling of carrier concentration and mobility in nitride heterostructures were performed in last decade [1-7]. The analysis of published theoretical and experimental data shows an importance of taking into account various factors on different scale levels such as lattice mismatch between layers, spontaneous and piezoelectric polarization, conduction bands shifts, barrier layer doping, interface roughness, alloy disorder and alloy clustering, Schottky barrier height, etc.

Carriers transport channels (2DEG) in the vicinity of heterointerface depend on the concentration of dopants in the barrier layer and on the presence of surface charge on the interface. Surface charge originates due to the atomic structure of wurtzite nitrides and is determined by spontaneous and piezoelectric polarization [1]. This can be approached at atomic level via *ab initio* calculations. Various mechanisms of carriers scattering can be considered at less detailed nanoscale level. In this paper we present multiscale approach which combines calculations on these two different scale levels. The results of our calculations of the dependence of 2DEG properties on various structure parameters such as Al molar concentration in barrier layer, barrier thickness, AlN layer thickness, spacer thickness are described in detail.

2 Multi-scale modeling scheme

The scheme of multi-scale semiconductor heterostructure modeling was developed in Dorodnicyn Computing Centre of RAS [8].

On the atomic level the system is described using crystallographic information and *ab initio* calculations performed in the framework of Density functional theory. First-principles modeling allows to determine electronic structure and basic properties of heterostructure, define polarization effects and calculate charge densities on the interfaces between layers. The results of modeling on the atomic scale level are used in the nanoscale level model for

© 2015 WILEY-VCH Verlag GmbH & Co. KGaA, Weinheim

the calculation of the charge carrier distribution in the heterostructure. At this level mathematical model contains the system of Schrödinger and Poisson equations.

$$-\frac{\hbar^2}{2}\frac{d}{dz}\left(\frac{1}{m^*(z)}\frac{d\psi}{dz}\right)+V(z)\psi(z)=E\psi(z),$$

$$\frac{d}{dz}\left(\varepsilon(z)\frac{d\phi}{dz}\right)=-e(N_D(z)-N_A(z)-n(z))+\sum_l \sigma_l\delta(z-z_l),$$

$$V(z)=-e\phi(z)+\Delta E_c(z),$$

$$n(z)=\sum_i(\psi_i(z))^2 n_i(z),$$

$$n_i(z)=k_BT\frac{m^*(z)}{\pi\hbar^2}\ln\left(1+\exp\left(\frac{E_F-E_i}{k_BT}\right)\right),$$

here z is the normal to the heterointerface coordinate, E_i and $\psi_i(z)$ are energetic levels and corresponding wavefunctions, $n(z)$ electron density, $\hbar$ Dirac constant, e electron charge, m^* effective electron mass, E_F Fermi level, $\phi(z)$ Coulomb potential, $V(z)$ potential energy of a carrier, N_D, N_A concentrations of donor and acceptor dopants, respectively, σ interface charge densities, δ delta-function, z_l coordinates of interfaces, ε dielectric constant, k_B Boltzmann constant, ΔE_c conduction band offset, and T temperature.

On the boundaries of the system (z=0, z=L, where L is the thickness of the whole heterostructure) the following conditions must be fulfilled:

$$\psi(0)=0,\ \psi(L)=0.$$

On the outer surface of the heterostructure where the barrier layer is placed the Schottky barrier height was defined: $\phi(0)=\phi_b$. The following expression for the Nickel contact was used: φ_b=1.3x+0.84.

On the left border the condition of electrical field absence was used: $\phi'(L)=0$.

Numerical solution of the problem allows us to obtain the electron density in the heterostructure. This information is used on the next level where the electron mobility and conductivity is calculated. The Mattheissen's rule is implemented at this level. The following scattering mechanisms are taken into account: optical and acoustic phonons, heterointerface roughness, remote modulation doping scattering, alloy disorder, dislocations, piezoelectric scattering. The formulas for relaxation times for different scattering mechanisms are given in [9]. All results are obtained for room temperature.

3 Modeling results as a function of Al concentration in barrier layer and of barrier thickness

In this series of computational experiments the molar concentration of Al and the barrier layer thickness for the structure without spacer and without doped barrier were varied. For the sake of definiteness the following values were assumed: dislocations concentration was taken equal to 3×10^9 cm^{-3}, interface roughness was taken equal to 1.2 nm, correlation length, 6 nm. Also the case was considered in which interface roughness was increasing with the increase of Al concentration in the barrier layer. Input data for numerical simulation such as dielectric constants for the materials, conduction band discontinuities, interface charge densities were calculated using approximation formulas given in [1].

It was taken into account that the maximum barrier thickness decreases with the increase of Al molar concentration to allow pseudomorphic growth of the barrier. Maximum barrier thickness should not be significantly larger than it's critical value which can be estimated by the formula: $t_{cr}\approx b_{ed}/2\varepsilon$, where b_{ed} = 0.3189 nm is the length of the Burgers vector for edge dislocations, ε the strain in a barrier, which depends on the Al concentration: $\varepsilon=(a_{GaN}-a_{AlGaN})/a_{AlGaN}$, a is the lattice constant. The dependence of critical value on the Al concentration (x) is shown in Fig. 1.

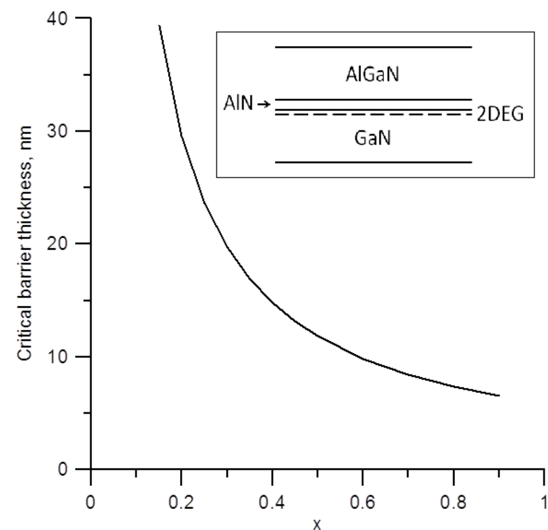

Figure 1 Dependence of critical barrier thickness on Al molar concentration. The schematic of AlGaN/AlN/GaN structure under consideration is pictured in the inset.

In Fig. 2 the effect of Al molar concentration in the barrier layer on the potential energy in heterostructure (a) and on the main wavefunction (b) is shown. The barrier layer thicknesses are equal to the critical values with respect to the corresponding x values. It is seen that with the increase of x the potential well depth also increases and the main energy levels move down (dashed lines in Fig. 2a). It is seen from Fig. 2b that in both cases Fang-Howard function [10] is a good approximation to the main wavefunction. It justifies the use of this approximation for the scattering intensity calculation.

 © 2015 WILEY-VCH Verlag GmbH & Co. KGaA, Weinheim

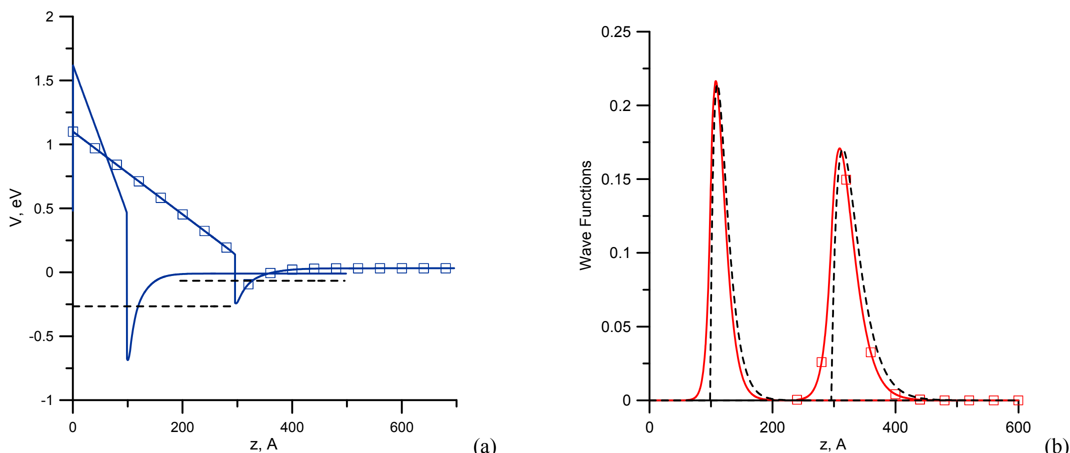

Figure 2 (a) Potential energy profiles in the heterostructure at various molar concentrations of Al in the barrier layer. Marked line, x=0.2. Solid line, x=0.6. Barrier thickness is equal to the critical value. (b) Wavefunctions (main) at various molar concentrations of Al in the barrier layer. Dashed line, Fang-Howard function. The designations are as seen in Fig. 2a.

Figure 3 shows the main integral properties of 2DEG dependence on the molar concentration of Al in the barrier layer. Barrier layer thicknesses are critical for the corresponding x values. According to expectations increasing x value leads to the increase of 2DEG electron concentration due to the increase of the spontaneous polarization. With the interface roughness parameters fixed as defined at the beginning of this paragraph increasing Al content above 0,15 leads to the lowering of the carrier mobility. This result is in agreement with previous modeling results [1].

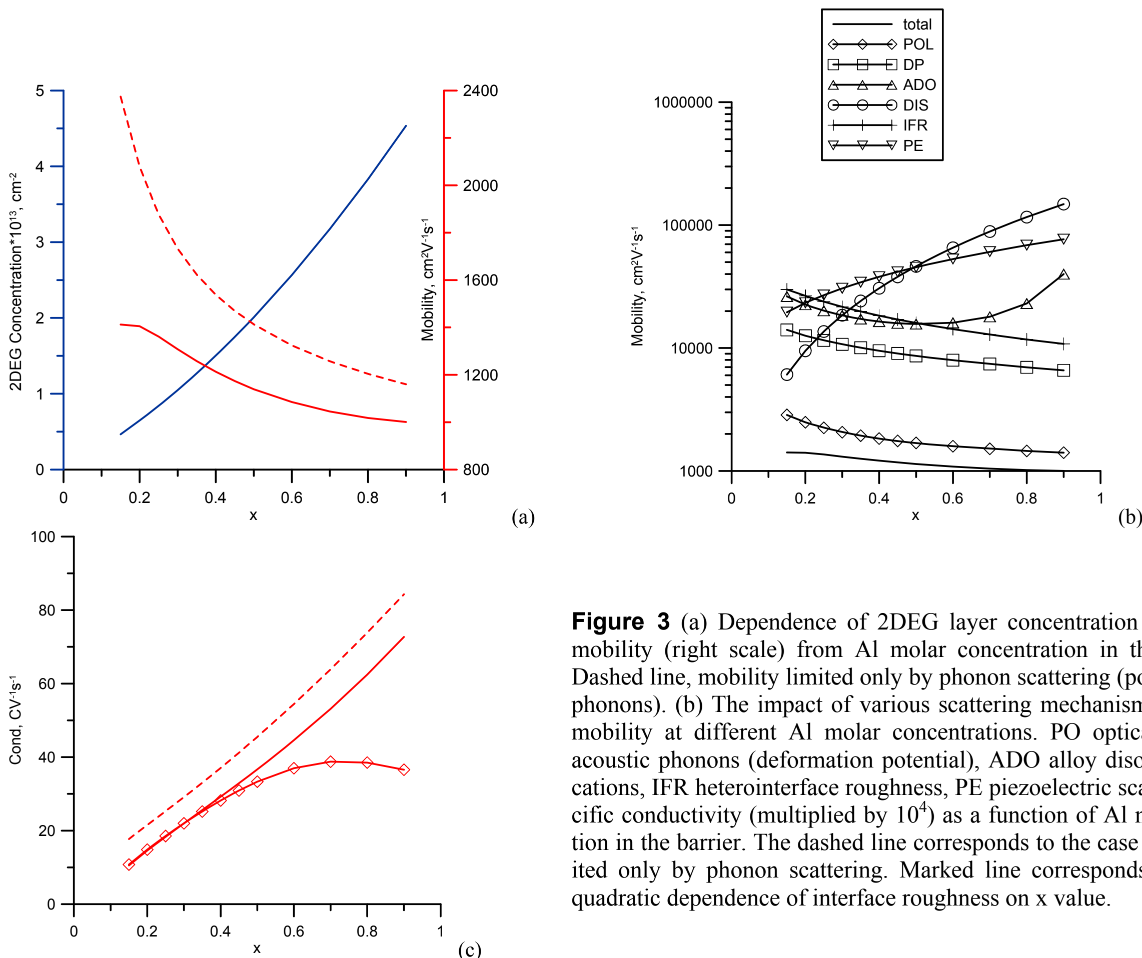

Figure 3 (a) Dependence of 2DEG layer concentration (left scale) and mobility (right scale) from Al molar concentration in the barrier layer. Dashed line, mobility limited only by phonon scattering (polar and acoustic phonons). (b) The impact of various scattering mechanisms on the carrier mobility at different Al molar concentrations. PO optical phonons, DP acoustic phonons (deformation potential), ADO alloy disorder, DIS dislocations, IFR heterointerface roughness, PE piezoelectric scattering. (c) Specific conductivity (multiplied by 10^4) as a function of Al molar concentration in the barrier. The dashed line corresponds to the case of mobility limited only by phonon scattering. Marked line corresponds to the case of quadratic dependence of interface roughness on x value.

© 2015 WILEY-VCH Verlag GmbH & Co. KGaA, Weinheim

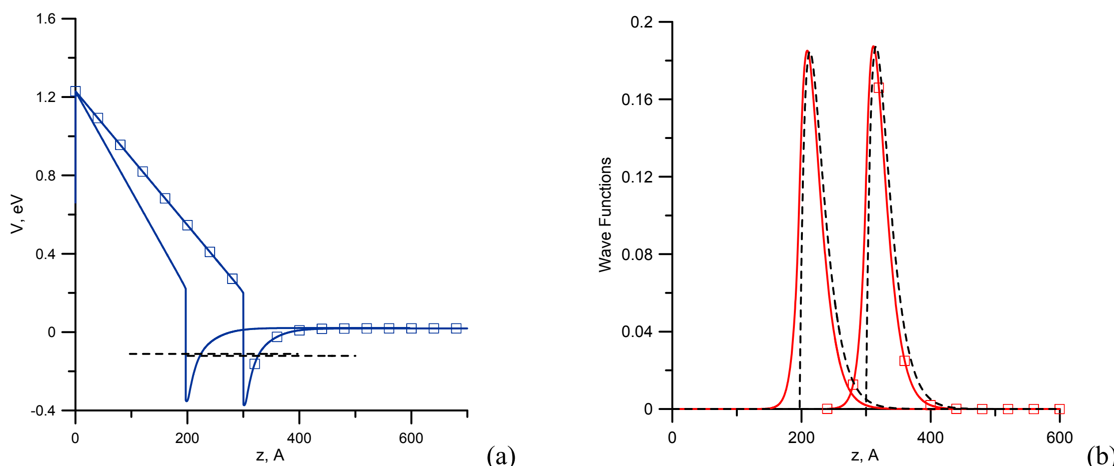

Figure 4 (a) Potential energy profiles in the heterostructure at various barrier layer thickness values. Marked line corresponds to the thickness of 30 nm. Solid line corresponds to the critical thickness. Al molar concentration in the barrier x=0.3. (b) Wavefunctions (main) at various barrier layer thickness values. Marked line corresponds to the thickness of 30 nm. Solid line corresponds to the critical thickness. Al molar concentration in the barrier x=0.3. Dashed line, Fang-Howard function.

The impact of various scattering mechanisms on the carrier mobility at different Al molar concentrations is shown in Fig. 3b. The first tendency is dominating, total conductivity increases with the increase of x value (Fig. 3c). Another case assuming that Al concentration growth leads to the quadratic growth of the interface roughness was considered (marked curve in Fig. 3c). In this case the appearance of the extreme point is possible on the conductivity curve.

The influence of the barrier layer thickness on the 2DEG properties was analyzed in a similar way. The results are shown in Fig. 4 and 5. The Al molar concentration in this case is constant: x = 0.3. The potential well depth increases with the growth of the barrier layer thickness, which leads to the increase of 2DEG carrier concentration. It in turn causes the decrease of their mobility. The main tendency here is that total conductivity increases with the growth of the barrier layer thickness. The limitation of the thickness by the pseudomorphic growth conditions is essential.

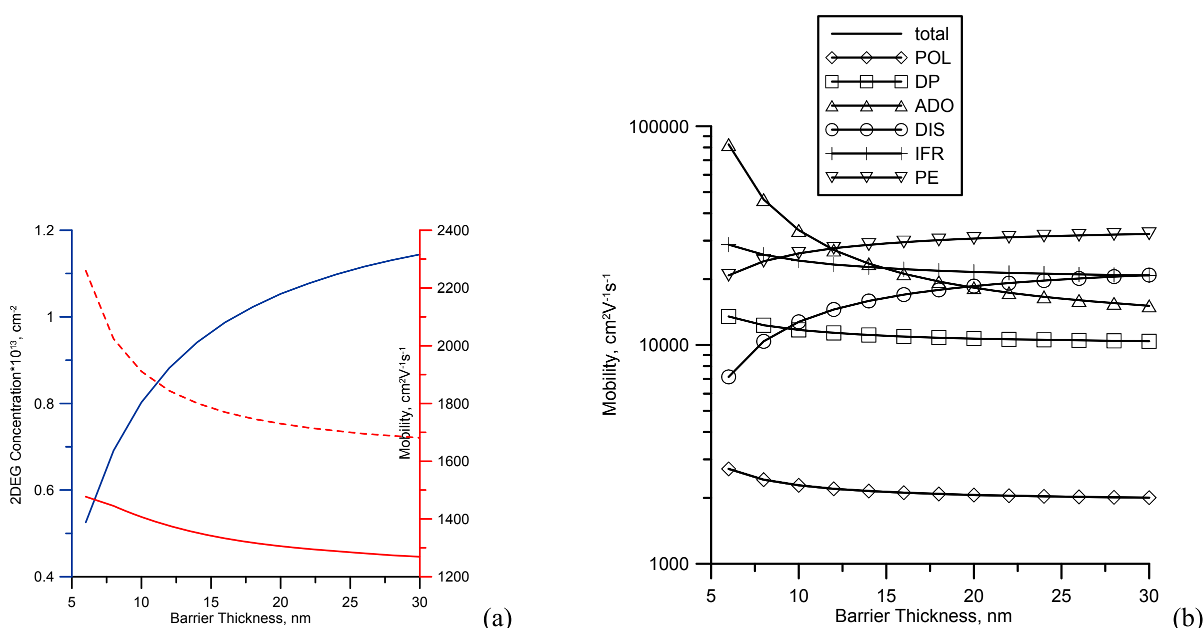

Figure 5 (a) Dependence of 2DEG layer concentration (left scale) and mobility (right scale) on various barrier thickness values. Dashed line, mobility limited only by phonon scattering (polar and acoustic phonons). Al molar concentration x=0.3. (b) The impact of various scattering mechanisms on the carrier mobility at different barrier thickness values.

 © 2015 WILEY-VCH Verlag GmbH & Co. KGaA, Weinheim

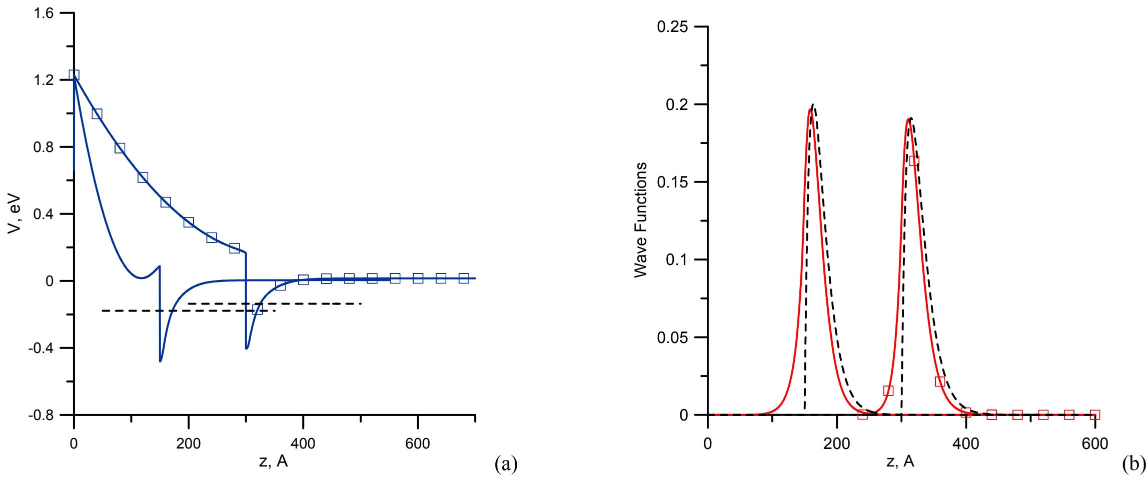

Figure 6 (a) Potential energy profiles in the heterostructure at various donor concentrations in the barrier. Marked line corresponds to the concentration of 10^{18} cm^{-3}. Solid line corresponds to the concentration of 10^{19} cm^{-3}. Al molar concentration in the barrier x=0.3. (b) Wavefunctions (main) at various donor concentrations in the barrier. The designations are as seen in Fig. 6a.

Figure 7 (a) Dependence of 2DEG layer concentration on spacer width at various barrier dopant concentrations. (1) 10^{18} cm^{-3}, (2) $5{\times}10^{18}$ cm^{-3}, (3) 10^{19} cm^{-3}, (4) $5{\times}10^{19}$ cm^{-3}. (b) Dependence of 2DEG carrier mobility on spacer width at various barrier dopant concentrations. The designations are as seen in Fig. 7a. (c) Dependence of 2DEG conductivity on spacer width at various barrier dopant concentrations. The designations are as seen in Fig. 7a.

© 2015 WILEY-VCH Verlag GmbH & Co. KGaA, Weinheim

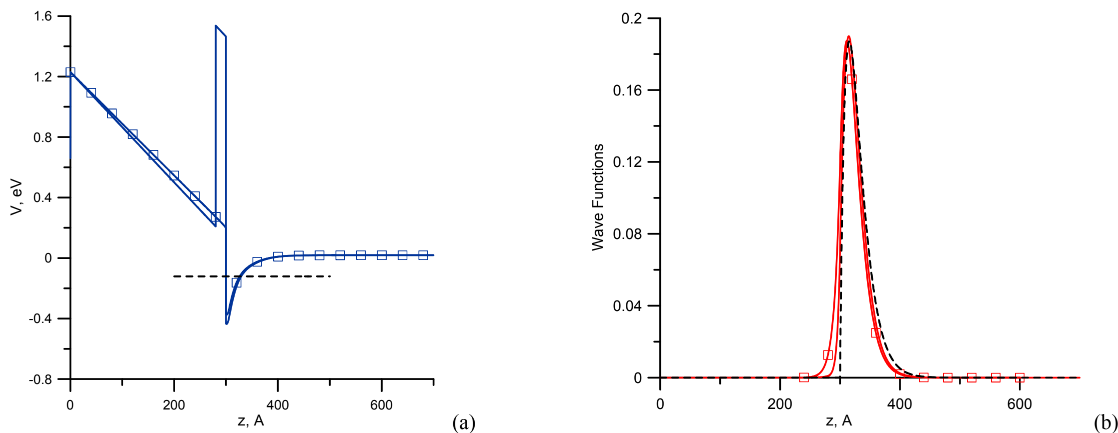

Figure 8 (a) Potential energy profiles in the heterostructure in the presence (solid line) and in the absence (marked line) of AlN layer. Al molar concentration in the barrier x=0.3. (b) Wavefunctions (main) in the presence (solid line) and in the absence (marked line) of AlN layer. Al molar concentration in the barrier x=0.3. Dashed line – Fang-Howard function.

4 Modeling results as a function of the level of barrier doping and of non-doped spacer width

The influence of the barrier layer doping is illustrated in Fig. 6a and b. In this case the thickness of non-doped spacer is zero, and Al mole concentration in the barrier layer equals to 0.3. It should be pointed out that growth of donor concentration in the barrier layer limits its thickness. Because otherwise bending of the conduction band in the barrier layer can reach Fermi layer (Fig. 6a), which would cause the formation of a high-electron concentration zone in the barrier layer. Thus, AlGaN layer thicknesses were different for various donor concentrations. The results of our calculations show that increase of dopant concentration in the barrier layer leads to the increase of 2DEG carrier concentration.

Dependence of 2DEG integral properties on the thickness of non-doped layer (spacer) at various dopant concentrations in the barrier layer are shown in Fig. 7. Obtained calculation results show that carrier concentration decreases and carrier mobility increases with the growth of the spacer thickness. Scattering on charge centers begins to play significant role in this case.

5 Modeling results as a function of the thickness of AlN layer in doped and non-doped structures

The influence of the thickness of AlN intermediate layer between barrier layer and 2DEG-channel is illustrated in Fig. 8 and 9. Here the interface charge density due to polarization effects was taken the same as without AlN layer. Therefore, it is assumed in the model that the AlN layer width is relatively small. Under this assumption appearance of the additional layer has almost no effect on the carrier concentration in 2DEG but causes slight changes in the electron density distribution in vicinity of the hetero-interface. In Fig. 8b it is seen that electron penetration under the barrier layer is weaker than in the case of structure without AlN layer. It leads to the weakening of the scattering on alloy disorder and to the increase of electron mobility with the growth of the AlN layer's thickness. This effect is more noticeable in the case of the barrier with dopants (Fig. 9b), when 2DEG carrier concentration is higher and the mobility is lower. In this case there is a maximum point on the dependence curve of total conductivity from the AlN layer thickness (Fig. 9c).

6 Summary

The computational multi-scale scheme for semiconductor heterostructure properties modeling was developed. It allows to calculate concentration and mobility of carriers in 2DEG. A number of computational experiments were performed to study the influence of such heterostructure characteristics as Al molar concentration in barrier, barrier thickness, barrier doping, spacer width, presence of AlN intermediate layer on the properties of 2DEG. It was shown that the following factors can cause the increase in carrier mobility: low Al molar concentration in barrier layer, increase of spacer width, presence of AlN intermediate layer between barrier layer and 2DEG-channel.

© 2015 WILEY-VCH Verlag GmbH & Co. KGaA, Weinheim

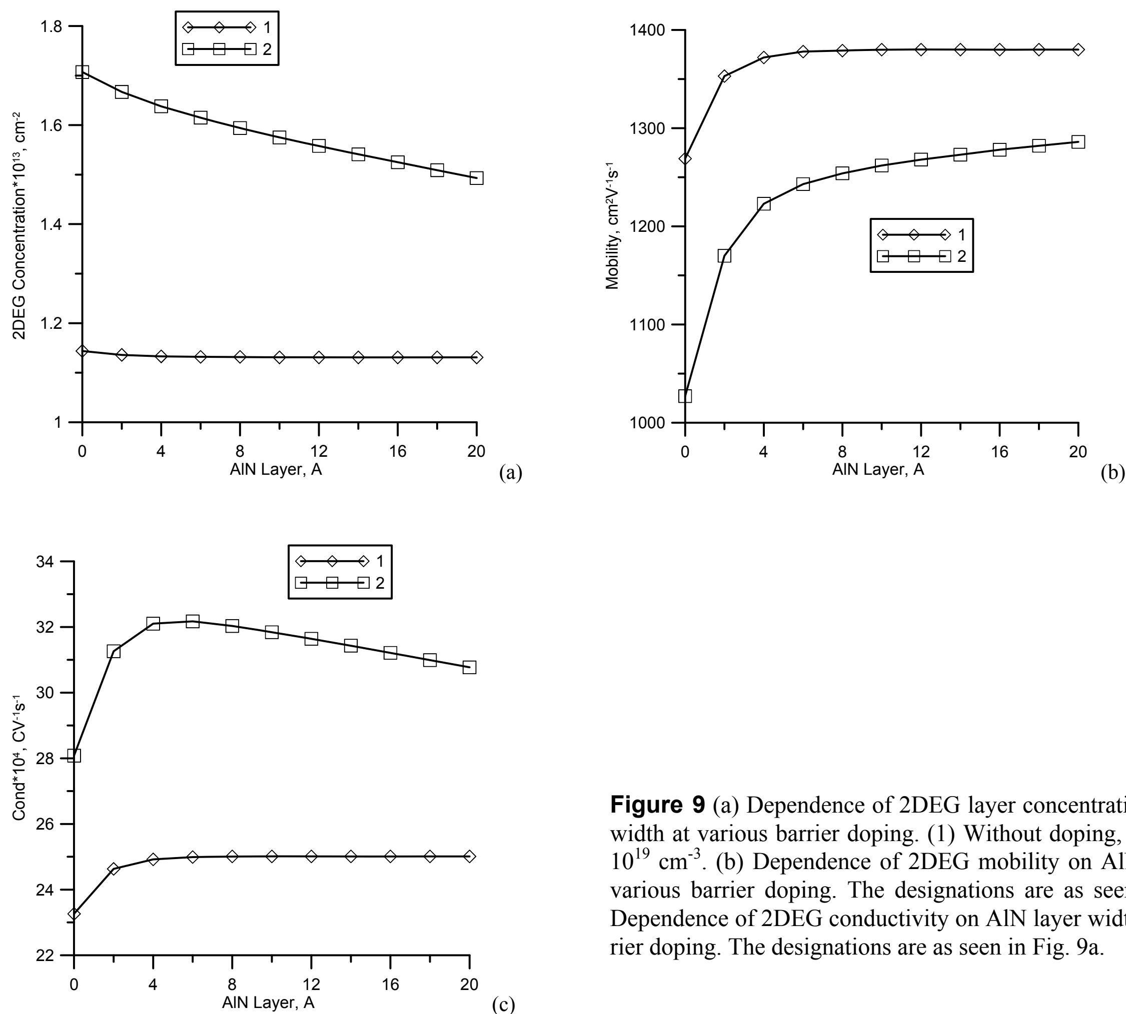

Figure 9 (a) Dependence of 2DEG layer concentration on AlN layer width at various barrier doping. (1) Without doping, (2) with doping, 10^{19} cm^{-3}. (b) Dependence of 2DEG mobility on AlN layer width at various barrier doping. The designations are as seen in Fig. 9a. (c) Dependence of 2DEG conductivity on AlN layer width at various barrier doping. The designations are as seen in Fig. 9a.

References

[1] O. Ambacher, J. Majewski, C. Miskys, A. Link, M Hermann, M. Eickhoff, M. Stutzmann, F. Bernardini, V. Fiorentini, V. Tilak, B. Schaff, and L. F. Eastman, J. Phys.: Condens. Matter **14**, 3399 (2002).

[2] D. Vasileska, S. M. Goodnick, S. Goodnick, Computational Electronics: Semiclassical and Quantum Device Modeling and Simulation (CRC Press, 2010).

[3] K. Tomizawa, Numerical Simulation of Submicron Semiconductor Devices (Artech House Inc., Japan, 1993).

[4] Z. Yarar, B. Ozdemir, and M. Ozdemir. Phys. Status Solidi B **242**, 2872 (2005).

[5] D. K. Ferry, S. M. Goodnick, and J. Bird, Transport in Nanostructures (Cambrige University Press, 2009), p. 659.

[6] H. Li, G. Liu, H. Wei, C. Jiao, J. Wang, H. Zhang, D.D. Jin, Y. Feng, S. Yang, L. Wang, Q. Zhu, and Z.-G. Wang, Appl. Phys. Lett. **103**, 232109 (2013).

[7] E. Ahmadi, H. Chalabi, S. W. Kaun, R. Shivaraman, J. S. Speck, and U. K. Mishra, J. Appl. Phys. **116**, 133702 (2014).

[8] K. Abgaryan, I. Mutigullin, and D. Reviznikov. Phys. Status Solidi C **12**, 460 (2015).

[9] D.Yu. Protasov, T.V. Malin, A.V. Tikhonov, A.F. Tsatsulnikov, and K.S. Zhuravlev, Semiconductors **47**, 33 (2013).

[10] F. F. Fang and V. E. Howard, Phys. Rev. Lett. **16**, 797 (1966).

© 2015 WILEY-VCH Verlag GmbH & Co. KGaA, Weinheim